EUROFUSION WP14ER-CP(16) 15739

J Morales et al.

The impact of the Boussinesq approximation on plasma turbulence in the scrape-off layer

Preprint of Paper to be submitted for publication in 43rd European Physical Society Conference on Plasma Physics (EPS)

This work has been carried out within the framework of the EUROfusion Consortium and has received funding from the Euratom research and training programme 2014-2018 under grant agreement No 633053. The views and opinions expressed herein do not necessarily reflect those of the European Commission.

The impact of the Boussinesq approximation on plasma turbulence in the scrape-off layer

J. Morales, B. Frei, F. Halpern, F. Musil, P. Paruta, P. Ricci, F. Riva, M. Siffert and C. Wersal

Swiss Plasma Center, EPFL, Lausanne, Suisse

Plasma turbulence in the tokamak scrape-off layer (SOL) region, where magnetic field lines intersect the reactor inner walls, determines the heat load on the limiter or divertor targets. This is one of the most crucial issues on the way towards a fusion reactor. Since SOL plasma is colder compared to the tokamak core, it is reasonable to use a fluid approximation to describe its dynamics. In particular the drift-reduced Braginskii equations are chosen to study the SOL plasma turbulence [1, 2]. To further simplify the drift-reduced Braginskii equations, the Boussinesq approximation is also applied in a number of numerical codes. This approximation consists in considering the plasma density constant in the evaluation of the divergence of the polarisation current, which simplifies substantially the solution of the Poisson equation necessary to evaluate the electric potential,

$$\nabla_\perp \cdot \left[\frac{nc}{B\omega_{ci}} \frac{d}{dt} \left(\boldsymbol{E}_\perp - \frac{\nabla_\perp P_i}{en} \right) \right] \approx \frac{nc}{B\omega_{ci}} \frac{d}{dt} \left(\nabla_\perp \cdot \boldsymbol{E}_\perp - \frac{1}{e} \nabla_\perp^2 T_i \right). \tag{1}$$

In this study, we first present a new formulation of the drift-reduced Braginskii equations and a new numerical implementation that allow us to relax the Boussinesq approximation in the GBS code [3, 4]. Second, we show the energy conservation properties of the new system of equations. Finally, we present the results of nonlinear three-dimensional turbulent simulations with and without the Boussinesq approximation.

Relaxation of the Boussinesq approximation

To relax the Boussinesq approximation in the GBS code we derive a new formulation of the vorticity equation. We start from the ion momentum equation given in [1],

$$m_i \frac{d}{dt} (n\boldsymbol{v}_i) + m_i (n\boldsymbol{v}_i) (\nabla \cdot \boldsymbol{v}_i) = -\nabla P_i - \nabla \cdot \overline{\overline{\boldsymbol{\Pi}}}_i + Zen \left(\boldsymbol{E} + \frac{1}{c} (\boldsymbol{v}_i \times \boldsymbol{B}) \right) - \boldsymbol{R}_i, \tag{2}$$

with the material derivative: $\frac{d}{dt} \equiv \frac{\partial}{\partial t} + (\boldsymbol{v}_i \cdot \nabla)$.

In a magnetised plasma the gyrofrequency is orders of magnitude larger than the typical turbulent frequencies $\partial/\partial t \approx (\rho_i^2/L_\perp^2)\, \omega_{ci} \ll \omega_{ci}$. Making use of this ordering and taking the cross product of Eq. (2) with the unit vector $\boldsymbol{b}$, we can evaluate the leading order perpendicular velocity. That is the $\boldsymbol{E} \times \boldsymbol{B}$ and the diamagnetic. Hence, at first order, the perpendicular velocity is $\boldsymbol{v}_{\perp i0} = \boldsymbol{v}_E + \boldsymbol{v}_{di} = c\frac{\boldsymbol{B}\times\nabla\phi}{B^2} + c\frac{\boldsymbol{B}\times\nabla P_i}{ZenB^2}$, with ϕ the electric potential ($\boldsymbol{E} = -\nabla\phi$). The polarisation velocity, defined as the difference between the ion velocity and the first order approximation

($\boldsymbol{v}_{pol} \equiv \boldsymbol{v}_{\perp i} - \boldsymbol{v}_{\perp i0}$) is a higher order term and can be approximated using the first order perpendicular velocities: $\boldsymbol{v}_{pol0} = \frac{1}{n\omega_{ci}}\boldsymbol{b} \times \frac{d}{dt}(n\boldsymbol{v}_{\perp i0}) + \frac{\left(\nabla\cdot\boldsymbol{v}_{\perp i0}+\nabla_{/\!/}v_{/\!/ i}\right)}{n\omega_{ci}}\boldsymbol{b}\times(n\boldsymbol{v}_{\perp i0}) + \frac{1}{nm_i\omega_{ci}}\boldsymbol{b}\times\nabla\cdot\overline{\overline{\boldsymbol{\Pi}}}_{i0}$. This reduction, called drift approximation, allow us to close the system of equations.

Neglecting the perpendicular component of the stress tensor (order $(\tau_i\omega_{ci}^2)^{-1} \ll 1$, with τ_i the ion collision time), the stress tensor can be expressed as: $\nabla\cdot\overline{\overline{\boldsymbol{\Pi}}}_{i0} = \nabla\cdot\overline{\overline{\boldsymbol{\Pi}}}_{FLR_i0} + \nabla\cdot\overline{\overline{\boldsymbol{\Pi}}}_{vis_i0}$. The second term on the right hand side is the divergence of the viscous stress tensor $\nabla\cdot\overline{\overline{\boldsymbol{\Pi}}}_{vis_i0} = G_0\boldsymbol{\kappa} - \frac{\nabla G_0}{3} + \boldsymbol{B}\nabla_{/\!/}\left(\frac{G_0}{B}\right)$, with the stress function $G_0 = -3\eta_0\left(\nabla_{/\!/}v_{/\!/ i} - \boldsymbol{\kappa}\cdot\boldsymbol{v}_{\perp i0} - \frac{\nabla\cdot\boldsymbol{v}_{\perp i0}}{3}\right)$.

Considering that the magnetic field varies on a length scale of order R (tokamak major radius), which is larger compared to the perpendicular turbulent length scale ($L_\perp/R \ll 1$), we simplify the finite Larmor radius (FLR) tensor that appears in the polarisation velocity. The following expression for the FLR tensor is retained: $\overline{\overline{\boldsymbol{\Pi}}}_{FLR_i0} = -m_in(\boldsymbol{v}_{di}\cdot\nabla)\boldsymbol{v}_i$. This form allows us to cancel the advection of the ion velocity by the diamagnetic component $\boldsymbol{v}_{di}$ (this is usually called the ‘gyro-viscous’ cancellation).

To obtain the vorticity equation we assume plasma quasi-neutrality ($n = n_e = n_i$). Or, equivalently, we consider the stationary charge conservation equation: $\nabla\cdot\boldsymbol{j} = 0$. The ion and electron continuity equations are used to obtain the vorticity equation: $\nabla\cdot\left(n\boldsymbol{v}_{pol0}\right) + \nabla_{/\!/}\left(\frac{j_{/\!/}}{e}\right) + \nabla\cdot(n(\boldsymbol{v}_{di} - \boldsymbol{v}_{de})) = 0$. Neglecting the compression of the $\boldsymbol{E}\times\boldsymbol{B}$ and diamagnetic velocities in the polarization expression (these terms are smaller by a factor $L_\perp/R \ll 1$), the first term on the left hand side writes

$$\nabla\cdot\left(n\boldsymbol{v}_{pol0}\right) = -\frac{1}{\omega_{ci}}\frac{\partial\Omega}{\partial t} - \frac{1}{\omega_{ci}}\nabla\cdot\left[(\boldsymbol{v}_E\cdot\nabla)\boldsymbol{\omega}\right] - \frac{1}{\omega_{ci}}\nabla\cdot\left[\nabla_{/\!/}\left(v_{/\!/ i}\boldsymbol{\omega}\right)\right] + \frac{1}{m_i\omega_{ci}}\nabla\cdot\left\{\boldsymbol{b}\times\left[G_0\boldsymbol{\kappa} - \frac{\nabla G_0}{3}\right]\right\}, \tag{3}$$

with Ω the new scalar vorticity: $\Omega = \nabla\cdot\boldsymbol{\omega} = -\nabla\cdot[\boldsymbol{b}\times(n\boldsymbol{v}_{\perp i0})] = \nabla\cdot\left(\frac{cn}{B}\nabla_\perp\phi + \frac{c}{ZeB}\nabla_\perp P_i\right)$ and $\boldsymbol{\omega}$ the perpendicular vector: $\boldsymbol{\omega} = -\boldsymbol{b}\times(n\boldsymbol{v}_{\perp i0}) = \frac{cn}{B}\nabla_\perp\phi + \frac{c}{ZeB}\nabla_\perp P_i$. The expression of the divergence of the polarisation velocity, Eq. (3), yields the new formulation of the vorticity equation:

$$\begin{aligned}\frac{\partial\Omega}{\partial t} &= -\frac{c}{B}\nabla\cdot\left\{\left[\phi,\boldsymbol{\omega}\right]\right\} - \nabla\cdot\left\{\nabla_{/\!/}\left(v_{/\!/ i}\boldsymbol{\omega}\right)\right\} + \omega_{ci}\nabla_{/\!/}\left(\frac{j_{/\!/}}{e}\right)\\ &\quad + \omega_{ci}\nabla\cdot(n(\boldsymbol{v}_{di} - \boldsymbol{v}_{de})) + \frac{1}{3m_i\omega_{ci}}\frac{B}{2}\left(\nabla\times\left(\frac{\boldsymbol{b}}{B}\right)\right)\cdot\nabla G_0.\end{aligned} \tag{4}$$

In this equation we use the Poisson bracket for the $\boldsymbol{E}\times\boldsymbol{B}$ advection term: $(\boldsymbol{v}_E\cdot\nabla)\boldsymbol{\omega} = \frac{c}{B}[\phi,\boldsymbol{\omega}]$ and the last term of Eq. (3) is written as a function of the curvature operator: $\frac{B}{2}\left[\left(\nabla\times\frac{\boldsymbol{b}}{B}\right)\cdot\nabla\right]$. The Poisson equation for the electric potential ϕ, $\nabla\cdot\left(\frac{cn}{B}\nabla_\perp\phi\right) = \Omega - \frac{c}{ZeB}\nabla_\perp^2 p_i$, is solved with an efficient parallel multigrid method in the GBS code.

Energy conservation with the new vorticity equation

Taking into account the continuity, parallel and temperature equations (for ions and electrons) together with the vorticity equation (4), we obtain the expression of the total energy of the system. A volume V is considered that does not exchange energy with the environment. The time derivative of the total energy integrated in the volume V yields

$$\begin{aligned}\frac{d}{dt}\int dV\left[\frac{nm_i}{2}\left(\boldsymbol{v}_{\perp i0}^2+v_{\parallel i}^2\right)+\frac{nm_e}{2}\left(\frac{j_\parallel}{en}\right)^2+\frac{3}{2}(p_i+p_e)+\frac{1}{8\pi}(\nabla_\perp\psi)^2\right]\\ =-\int dV\left[\frac{j_\parallel^2}{\sigma_\parallel}+\frac{G^2}{3\eta_0}\right]+\varepsilon\end{aligned}\quad(5)$$

with

$$\begin{aligned}\varepsilon=\int dV\left[m_i\boldsymbol{v}_{\perp i0}^2\left(\frac{c}{2Ze}\nabla p_i+cn\nabla\phi\right)\right]\cdot\left\{\nabla\times\frac{\boldsymbol{b}}{B}\right\}\\ +\int dV\left[\frac{mm_i}{2}\boldsymbol{v}_{pol}\cdot\nabla\left(\boldsymbol{v}_{\perp i0}^2+v_{\parallel i}^2\right)+\frac{3}{2}\boldsymbol{v}_{pol}\cdot\nabla p_i\right].\end{aligned}\quad(6)$$

The time evolution of the total energy, left hand side of Eq. (5), varies because of the Joule and viscous dissipation. Also it changes because of the approximation made in the drift reduction of the Braginskii equations (ε term). This error is split into two terms in Eq. (6), the first one is a curvature term, smaller than the first term on the left hand side of Eq. (5) by a factor $L_\perp/R \ll 1$. The second term of Eq. (6) is of order $(\boldsymbol{v}_{pol}\cdot\nabla)$. By comparing this last term with the corresponding term on the left hand side of Eq. (5), (d/dt), we obtain: $\boldsymbol{v}_{pol}\cdot\nabla \approx \frac{\rho_i^2}{L_\perp^2}c_s\frac{1}{L_\perp} \approx \frac{\rho_i^2}{L_\perp^2}\frac{\rho_s\omega_{c_i}}{L_\perp} = \frac{\rho_s}{L_\perp}\frac{d}{dt} \ll \frac{d}{dt}$. Therefore, if the dissipation terms can be neglected, the new model conserves the total energy within the ordering used for its deduction.

Numerical results

With the GBS code we perform turbulent simulations taking into account the Boussinesq (B) and the new non-Boussinesq (NB) model. In these simulations we vary the safety factor q and the ratio between ion and electron temperatures at the last closed flux surface, $\tau = T_{i0}/T_{e0}$. We consider cold ions ($\tau = 0$) and a hot ion regime ($\tau = 2$).

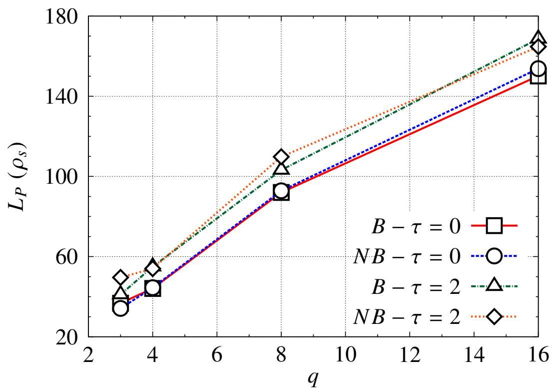

Figure 1: Radial pressure length (ρ_s units) as a function of the safety factor q.

The SOL pressure typical radial length is defined as $L_P = \left\langle \left|\frac{1}{P}\frac{\partial P}{\partial r}\right|^{-1}\right\rangle$. This quantity is averaged in time during the turbulent quasi-steady state. In Fig. 1 we plot the value of L_P as a function of q for different simulations with and without the Boussinesq approximation. For the simulations with $\tau = 0$ the difference between the Boussinesq and the non-Boussinesq model is of the order of a few percent. On the other hand, for $\tau = 2$ and $q = 3$, the L_P value for the non-Boussinesq case is approximatively 20% larger compared to the value obtained with the Boussinesq approximation. In the following we will focus our analysis on the latter case ($\tau = 2$ and $q = 3$).

In Fig. 2 we present the pressure profiles for the B and NB models. In this figure a flattening of the pressure profile is visible for the NB case. The poloidally averaged profile and the pressure profile at the low field side (LFS) of the tokamak are shown. This flattening, or increase of L_P, can be explained by the enhancement of the turbulent transport. This is illustrated in Fig. 3 where the radial profile of the standard deviation and the skewness of the pressure field are plotted. In these two figures we observe that both quantities have larger values if the NB model is considered. This indicates that the turbulent fluctuations increase if the Boussinesq approximation is relaxed for a low q and when $T_{i0} > T_{e0}$.

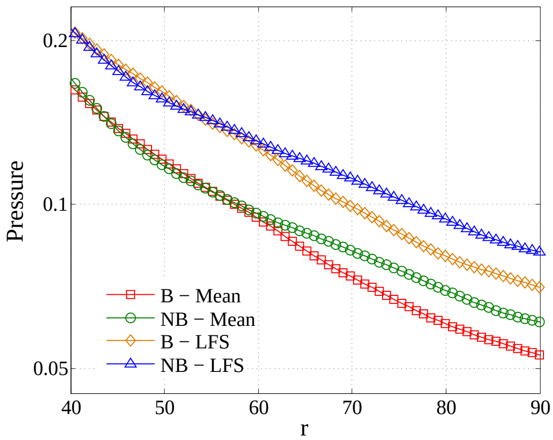

Figure 2: Radial pressure profile (semi-logarithmic plot) at the SOL, poloidal mean profile and profile at the low field side (LFS), for $q = 3$ and $\tau = 2$.

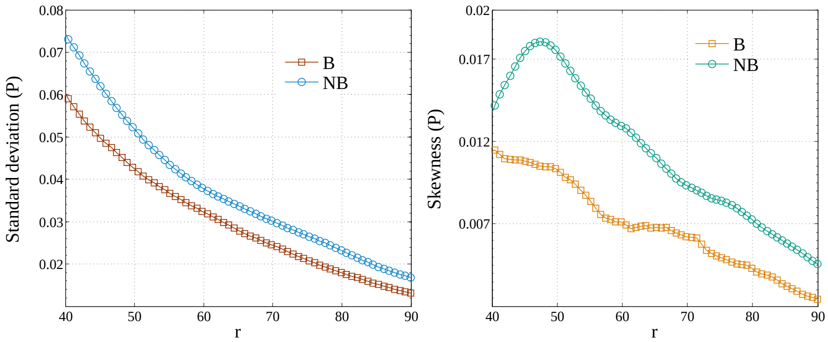

Figure 3: Standard deviation (left) and skewness (right) of the pressure field as a function of the radius, for $q = 3$ and $\tau = 2$.

Finally, in Fig. 4, the spectrum of the pressure field is displayed. We observe that for the NB case the pressure fluctuations are higher and are concentrated at lower poloidal mode numbers. This confirms the previous observation, the L_P value is higher because turbulent fluctuations are enhanced if the Boussinesq approximation is relaxed. Investigation are currently ongoing to understand if this is the result of the increase of the linear growth rate of the main instability in the NB model and/or the result of a more complex nonlinear mechanism.

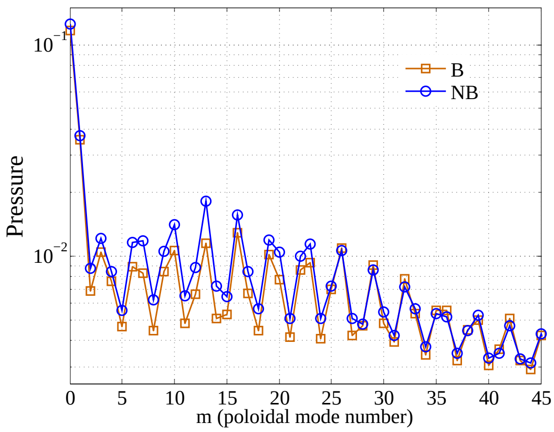

Figure 4: Pressure spectrum.

This work has been carried out within the framework of the EUROfusion Consortium and has received funding from the Euratom research and training programme 2014-2018 under grant agreement No 633053. The views and opinions expressed herein do not necessarily reflect those of the European Commission.

References

[1] S.I. Braginskii, Rev. P. Phys. **1**,205 (1965)
[2] A. Zeiler, Max-Planck-Institute, IPP 5/88 (1999)
[3] P. Ricci *et al.*, P. Phys. Cont. Fusion **54**,124047 (2012)
[4] F. Halpern *et al.*, J. Comp. Phys. **315**,388 (2016)